Polymer Journal

REVIEW ARTICLE

Special Issues –International Symposium on Polymer Crystallization 2007–

Colloidal Crystallization As Compared with Polymer Crystallization

By Tsuneo OKUBO[1,2*]

Recent work made in the author's laboratory on the morphology (especially, giant colloidal crystals), crystal structure, fundamental properties such as phase transition, light-scattering, viscosity and elasticity, crystallization kinetics and electro-optics of colloidal crystals have been reviewed. Colloidal crystals are really crystal as typical other crystals, metals, polymers and ice, for example. However, the inter-particle force of colloidal crystal is "repulsion" exclusively and being different from the other typical crystals, where the inter-particle "attraction" plays an important role for crystallization. It is pointed out that the apparent "attraction" is induced inevitably for the colloidal crystallization in a closed vessel.

KEY WORDS: Colloidal Crystal / Colloidal Spheres / Inter-particle Electrostatic Repulsion / Crystal Structure / Light-scattering / Rigidity /

Recently, keen attention has been paid for the colloidal crystals, *i.e.*, crystal-like distribution of colloidal particles in suspensions of aqueous and organic solvents.[1–13] Many researchers have studied structural colors, inter-particle interaction, crystal structure, morphology of single crystals, phase transition, crystallization kinetics of nucleation and crystal growth, physico-chemical properties (rigidity, viscosity, etc.), structural change induced by the external fields such as gravity, centrifugal and electric fields, shearing forces, and technical application (photonic crystals and electro-optic devices, etc.).

Two groups of colloidal crystals have been studied hitherto: those in (i) diluted and deionized aqueous suspensions[14–26] and (ii) concentrated suspensions in the refractive index matched organic solvents.[27–32] The formers are very convenient models for both the *soft* and *hard* sphere systems, depending on the ionic concentrations of suspension, *i.e.*, *soft* crystals in the exhaustively deionized state and *hard* crystals in the presence of rather large amount of sodium chloride, for example.

Generally speaking, most colloidal particles in water get negative charges on their surfaces by two mechanisms: by the dissociation of ionizable groups and by the preferential adsorption of ions from suspension. These ionic groups leave their counter-ions, and these excess charges accumulate near the surface, forming an electrical double layer. The counter-ions in the diffuse region are distributed according to a balance between the thermal diffusive force and the forces of electrical attraction with colloidal particles. The importance of the electrical double layers for the colloidal crystallization has been clarified by many researchers.[1–26] Giant size of single crystals has been formed in the exhaustively deionized and diluted suspension of colloidal spheres. Colloidal crystals are very beautiful and fantastic from their strong structural colors, because the inter-particle distance is just in the range of the light wavelength and each single crystal reflects light in different colors by the Bragg diffraction.

In this article the general features of colloidal crystals in terms of their structural, kinetic, and dynamic properties such as morphology, crystallization kinetics, physico-chemical properties, and electro-optics phenomena are reviewed.

WHY CRYSTAL STRUCTURES ARE FORMED

Colloidal crystallization takes place for monodispersed colloidal particles in suspension. Many researchers have clarified that the colloidal crystals are formed by Brownian movement of colloidal size of particles that results from inter-particle repulsion according to the principle of minimizing dead space.[11,20,25] In other words, particles form crystal-like distribution automatically with the help of Brownian movement of particles by maximizing packing density.

When extra repulsive interaction, like electrostatic repulsion, is in effect among colloidal particles in addition to the repulsion forces from their *Brownian movement*, colloidal crystallization takes place easily even at the very low particle concentrations. The thickness of the electrical double layers is estimated approximately with the Debye-screening length, D_l, given by eq 1. Debye length corresponds to the distance from the colloidal surface, where the electrostatic potential decreases to be 1/2.7 compared to that at the slipping zone.

$$D_l = (4\pi e^2 n/\varepsilon k_B T)^{-1/2} \quad (1)$$

Here, e is the electronic charge, and ε is the dielectric constant of the solvent, n is the concentration of "diffusible" or "free-state" cations and anions in suspension. Thus, n is the sum of the concentrations of diffusible counter-ions, foreign salt and both H^+ and OH^- from the dissociation of water. Maximum

[1]Institute for Colloidal Organization, Hatoyama 3-1-112, Uji 611-0012, Japan
[2]Cooperative Research Center, Yamagata University, 4-3-16 Johnan, Yonezawa 992-8510, Japan
*To whom correspondence should be addressed (Tel/Fax: +81-774-32-8270, E-mail: okubotsu@ybb.ne.jp).

 doi:10.1295/polymj.PJ2007182

Polymer Journal

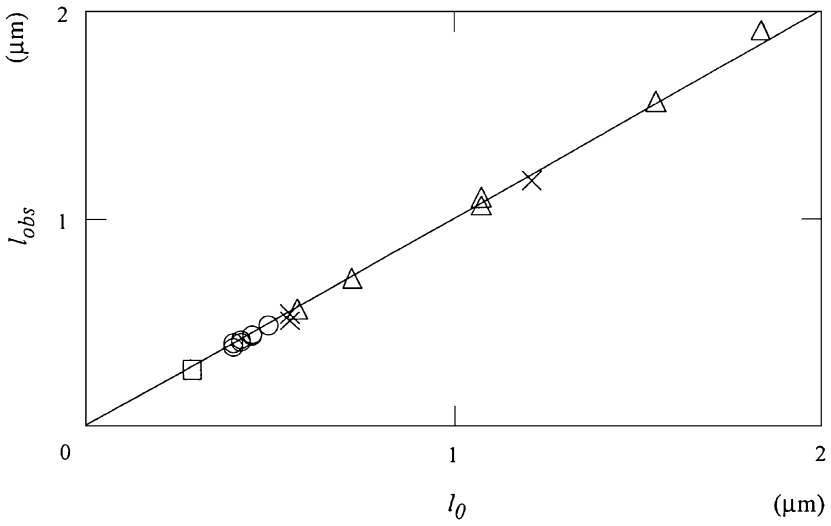

Figure 1. Comparison of the nearest-neighbored interparticle distances observed (l_{obs}) with the calculations from the sphere concentration (l_o). ○, □: from the reflection spectroscopy, ×, △: light-scattering measurements.

value of D_l in water is *ca.* 1 μm, which is estimated from eq 1 by taking $n = 2 \times 10^{-7}$ (M) $\times N_A \times 10^{-3}$ cm^{-3}, where N_A is the Avogadro number. It should be noted that the electrical double layers are formed always without exception in the colloidal dispersions of a solid in a polar liquid.

In the deionized state, electrical double layer is very thick, and the inter-particle repulsive forces prevail over a long distance, as long as micrometers, though the forces become very weak. Formation of the crystal-like ordering is explained nicely with the *effective soft-sphere model*. The effective diameter, d_{eff} of spheres includes the Debye-screening length, D_l, and given by the diameter plus twice the Debye length. When d_{eff} is shorter than the observed inter-sphere distance, l, a gas-like distribution is observed. When d_{eff} is comparable to or a bit shorter than the inter-sphere distance, the distribution of spheres is usually liquid-like. When the effective diameter is close-to or larger than the observed inter-sphere distance, crystal-like ordering occurs. The effective soft-sphere model has been supported by many researchers from the systematic comparison of d_{eff} with l values.[11,20,25]

Figure 1 demonstrates clearly that the lattice spacing of colloidal crystals changes according to the particle concentration exclusively, which supports strongly the importance of the inter-particle repulsion induced by Brownian movement of particles themselves and also the electrostatic inter-particle repulsive forces. Itano *et al.*[33] have reported that the Coulomb crystals are formed for the trapped spherical plasma with a single sign (plus) of charge. This observation supports strongly the important role of the *electrostatic repulsion forces* for the crystallization in addition to the *Brownian movement* of the respective plasmas.

MOTPHOLOGY AND CRYSTAL STRUCTURE OF COLLOIDAL CRYSTALS

Figure 2 shows close-up color photographs of the single crystals that appeared in the aqueous dispersions of monodispersed silica spheres. These suspensions were deionized exhaustively by the coexistence of cation- and anion-exchange resins more than three weeks. Cells were quartz glass optical cell for fluorescence measurements, 10 mm in width, 10 mm in depth and 40 mm in height (Figure 2(a)) and a test tube (Figure 2(b)). The resins coexisted in the bottom of the cell (the picture of the bottom is cut here). The pictures were taken 7 d and 18 d after suspension preparation, and 40 min and 1 h after inverted mixing, respectively. Sphere concentrations were 0.00095 and 0.00083, respectively, in volume fraction. In these experimental conditions, very few nuclei are formed and the single crystals become very large. These single crystals can be observed with the naked eye, and they are quite beautiful. It should be noted that formation of the single crystals is quite similar to metals. In other words, morphology of colloidal crystal is quite the same as that of other typical crystals. Most

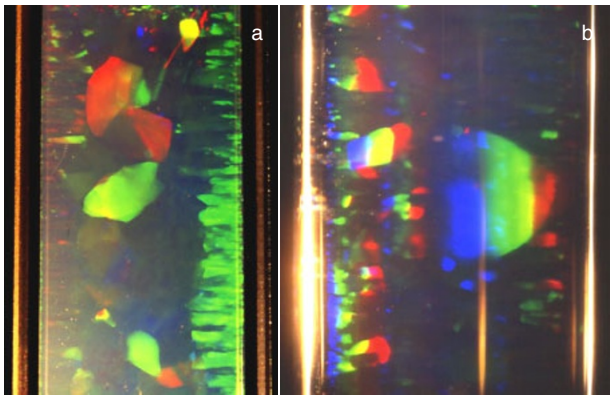

Figure 2. A Close-up color pictures of colloidal crystals of (a) silica spheres (103 nm in diameter) in a plane cell and of (b) silica spheres (110 nm) in a test tube (12 mm in outside diameter). (a) $\phi =$ 0.00095, with ion-exchange resins, 7 d after suspension preparation, 30 min after inverted mixing, (b) $\phi = 0.00083$, 18 d after preparation, 1 h after mixing.

SPECIAL ISSUE

metal crystals are composed of single crystals surrounded by the grain boundaries. Lattice spacing of colloidal crystals, which is studied with reflection spectroscopy in detail,[25] is very long–several thousand times greater compared with that of metals- and just in the range of light wavelengths. There are two kinds of single crystals, which are observable in the picture. Red, blue, yellow, and block-like ones are formed by the homogeneous nucleation mechanism in the bulk phase far from the cell wall. Green and pillar-like crystals grow by the heterogeneous nucleation mechanism along the cell wall. It should be noted that each single crystals are surrounded by grain boundaries and packed densely.[34] When the incident light angle is changed slowly, packed state of the single crystals is observable.[34]

Size of single crystals increased when sphere concentration decreased in the exhaustively deionized suspensions.[11,20,23] This observation is quite understandable, because crystal size should increase with decreasing nucleation rate, and also with decreasing number of nuclei. Nucleation rate, of course, decreases as sphere concentration decreases. When the sphere concentration is comparatively high, size of colloidal crystals is very small, and single crystals are not observed with the naked eye at all.

Generally speaking, crystal structures are face-centered cubic (*fcc*) or body-centered cubic (*bcc*) lattices. Square-ordered structures, however, were observed when two plates of a cell were oriented in a wedge geometry.[7] From much data on the colloidal lattice structures, it is concluded that the *fcc* lattices are most stable and they transform into bcc lattices when 1) particle concentration is highly diluted, 2) a small amount of salt is added, 3) the suspension temperature is raised, 4) charge density of particles is high, or 5) high pressure is applied.[11,20] Coexistence of *fcc* and *bcc* crystal lattices is highly related to the increased free space for particles forming lattice structures, *i.e.*, the *fcc* form is more dense than the bcc. The *fcc* and *bcc* structures are observable visually by a metallurgical microscope, especially in sedimentation equilibrium, and the interparticle distances can be determined from microscopic observation. However, it is usually difficult to observe the three-dimensional lattice structures from microscopy, even scanning microscopy.

Amorphous-solid (or glass) structures are observed for highly polydispersed colloids, especially in rather concentrated suspensions. Several types of asymmetrical colloidal crystals have been studied, especially in sedimentation equilibrium in deionized suspensions of anisotropic-shaped particles. Cylindrical colloids of nickel dimethylglyoxime (9.6 µm in length, 0.12 µm in diameter) were ordered in a hexagonal array.[35] It is clear that the particles are oriented to reduce the dead space as effectively as possible. Bowl-shaped polystyrene particles also oriented in deionized suspension.[36,37] Interestingly, these particles included spheres of various sizes in their cavities. Both the host and guest particles were not in direct contact, but were kept apart from each other by the electrical double layers formed around the particles. The transformation of the particle distribution of ellipsoidal poly(tetrafluoroethylene) from unsymmetrical to symmetrical crystals has been observed, with dilution accompanied by the thickening of the electrical double layers.[37] Asymmetrically ordered structures, similar to paved bricks, have been formed in rectangular tungstic acid colloids.[37] Ordered phases of plate-like particles were observed in concentrated dispersions.[37]

Alloy structures of colloids are especially important because most of the structures of metal alloys also appear in colloidal suspensions of binary mixtures of spheres of different sizes. The superlattice structures observed hitherto in colloidal systems are of the AlB_2, $NaZn_{13}$, $CaCu_5$, $MgCu_2$, NaCl, and AB_4 types.[20] Note that these alloy structures are explained by changes in the effective size ratio, *i.e.*, effective size of small spheres, including the electrical double layers *vs.* that of large spheres and the segregation effect. The author's group clarified the cationic charged colloidal crystals are formed though the spheres are not so stable chemically in the deionized condition.[38] Furthermore, core-shell type spheres formed colloidal crystals in deionized aqueous media.[38] Zhu *et al.*[39] reported morphological properties of the colloidal crystals of the hard-sphere systems in microgravity using Space Shuttle Columbia.

Here, we should discuss why the morphology of colloidal crystals formed by the electrostatic *repulsion* is quite similar to those of typical crystals governed by the inter-particle *attraction* forces. We should note that the colloidal crystallization takes place in a closed vessel. Even air-suspension interface the crystal suspension is closed by the interfacial tension. In this closed condition, *inter-sphere repulsion* is transmitted to the *effective intersphere attraction* as is shown in Figure 3 schematically. However, of course, the original inter-sphere forces are repulsion exclusively.

CRYSTALLIZATION KINETICS

Most kinetic measurements on colloidal crystallization showed an induction period, after which the crystal growth starts, especially in diluted suspensions. This observation supports that the kinetics of colloidal crystallization is explain-

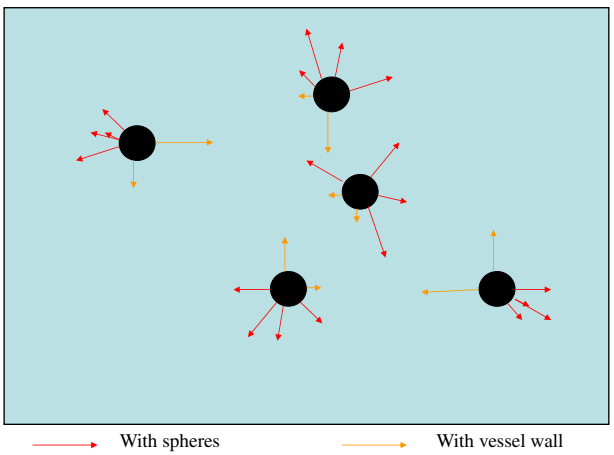

Figure 3. The effective inter-particle "attraction" is induced from the inter-particle "repulsion" inevitably in a closed vessel with a help of Brownian translational movement of each particles.

able by the classical diffusive crystallization theory, including nucleation and crystal growth processes.[40–43]

The number of nuclei that germinate per unit of time, the nucleation rate, v_n, is given by

$$v_n = N_n/t_i, \tag{2}$$

where N_n is the total number of nuclei formed during the nucleation process and t_i is the induction period and corresponds to the time of nucleation process. Here, we assume that the number of nuclei equals the number of single crystal, N_c, is given for a cubic lattice by

$$N_c = \sqrt{2}L^3/l^3, \tag{3}$$

where L and l are the mean size of single crystals formed and the nearest-neighbor inter-sphere distance, respectively. Total number of colloidal spheres (N_T) in a unit volume is $\phi/[(4/3)\pi(d_o/2)^3]$. Here, d_o is the diameter of sphere particles. Then v_n is given by

$$v_n = N_T/N_c t_i = \phi l^3/[(4\sqrt{2}/3)\pi(d_o/2)^3 L^3 t_i], \tag{4}$$

where ϕ is the volume fraction of sphere particles.

The size of colloidal single crystals formed from the homogeneous nucleation, L, is estimated from the peak intensity, I, of the reflection spectra;[29]

$$I \propto N_{cryst} L^3 \propto L^3 \tag{5}$$

where N_{cryst} is the number of single crystals in the reflection volume, which is directly proportional to the number concentration of crystals in the final stages of the crystallization process, being equal to the total number of nuclei formed in the whole course of crystallization.

Colloidal crystallization processes are composed of the fast growth of a meta-stable crystal (step 1) and the slow reorientation toward the stable crystal (step 2). The first crystal growth rate of a meta-stable crystal, v_1, is given by[43]

$$v_1 = v_{1\infty}[1 - \exp(-\sigma)]. \tag{6}$$

Here, σ is the relative super-saturation given by $(\phi - \phi_c)/\phi_c$. ϕ_c is the critical concentration of melting. $V_{1\infty}$ Is the maximum crystal growth rate eq 6 is further simplified as

$$v_1 = v_{1\infty} - v_{1\infty}\phi_c/\phi. \tag{7}$$

Eq 7 means that the growth rate should decrease linearly as the reciprocal sphere concentration increases, which was supported experimentally, but only in a very low sphere concentration range.[43]

The peak in the reflection spectroscopy became sharp with time in the course of crystallization, which corresponds to an increase in crystal size. The background intensity decreased in the course of crystallization, which is ascribed to the diminution in the multiple scattering of the suspension. The peak shift reflects the fact that metastable and loose crystals are formed in the first crystallization step and then the crystals become stable and compact. The nearest-neighbor intersphere distance, l is determined from λ_p using eq 8 in aqueous suspension at the reflected angle of 90° and 25 °C.[44]

$$l = 0.460 l_p \tag{8}$$

Calculated value of the nearest-neighbor inter-sphere distance, lo, on the other hand, is obtained from eq 9 in the same conditions as eq 8:[44]

$$l_o = 0.904 \mathrm{d}_o \phi^{1/3} \tag{9}$$

As was described earlier, an excellent agreement between l and l_o has been obtained, which demonstrates that the lattice spacing of the colloidal crystal changes according to the sphere concentration exclusively, and furthermore, that the crystals are formed by inter-sphere repulsion from the Brownian movement of the spheres themselves and also by the electrostatic inter-sphere repulsive forces.

The nucleation rate, v_n was estimated using eq 2 to eq 4 and observed t_i. v_n increased substantially as sphere concentration increased. v_n increased by 10^{10}-fold when ϕ increased by 10^2-fold. An increase in sphere concentration is followed by an increase in v_n, and number of nuclei (N_n), and resulted in a decrease in the size of single crystals formed, as discussed by Dhont *et al.*[29] It should be mentioned here that the size of single crystals, observed with the naked eyes, is polydisperse as has often observed.[23] Therefore, the clear separation of the nucleation step from the crystallization process will be difficult, and the nucleation reaction may remain operative even in the crystal growth period.

The fast and slow crystal growth rates, v_1 and v_2, were evaluated for colloidal crystallization. v_1 increases first from 5 μm/s to 20 μm/s and then decrease back to 5 μm/s, passing a maximum. The v_1-values above $\phi = 0.01$ remain 5 μm/s and are quite insensitive to sphere concentration. It should be mentioned here that the v_1-values in the diluted suspensions decrease linearly as the reciprocal concentration of spheres increases.[41] A clear explanation for the crystallization rate first going up and then going down as sphere concentration increases has not yet been obtained. However, the main cause will be the dynamic nature of phase transition, *i.e.*, spheres in the colloidal lattices interacting strongly with each other, and further, in a cooperative manner through the electrical double layers. This dynamic phase transition is different from the classical explanation, which is the transitional diffusion of monomers. It should be noted here that the importance of the dynamic phase transition has been reported for colloidal crystals and for other crystals such as metals and polymers.

The slow step of crystallization decreases very sharply as sphere concentration increases. v_2 decreases from 3 μm/s to 0.7 nm/s when ϕ increases from 0.004 to 0.04. The second slow crystallization step is ascribed to the reorientation of the metastable crystals formed in the first step toward the stable ones matched with the other crystals mediated by the grain boundaries and the cell wall. When sphere concentration is high, the number of the meta-stable crystals formed is huge and their size becomes quite small. Then, a very long time will be required for the crystals to be matched with other crystals and cell wall. The occurrence of Ostwald ripening is also highly plausible in the slow process, though direct observation was not

successful until Wong *et al.*[45] observed the ripening for colloidal crystallization processes.

Kinetic analyses of colloidal crystallization in alcoholic organic solvents and their aqueous mixtures have been studied by reflection spectroscopy.[46] The kinetic study of colloidal crystallization has been made for the silica spheres modified with polymers on their surfaces in acetonitrile.[47] Colloidal crystallization has been studied kinetically in microgravity, produced by parabolic flights of an aircraft.[48] Crystal growth rates decreased in microgravity by about 25% compared with those in normal gravity. One of the main causes for the retardation in microgravity was suggested to be elimination of the downward diffusion of spheres, which may enhance the inter-sphere collisions. No convection of the suspensions in microgravity was also or much more important than the elimination effect of the downward diffusion. Crystal growth rates of the colloidal alloys of binary mixtures of monodispersed polystyrene and/or silica spheres have been studied in microgravity.[49] The rates increased substantially up to *ca.* 1.7 folds in microgravity compared with those in normal gravity. We should note that the *segregation* effect is familiar for binary mixtures of colloid and powder science, large spheres are segregated upward and small ones downward in normal gravity. In microgravity such segregation disappears and the homogeneous mixing takes place favorably, which leads fast alloy crystallization. The author studied the kinetics of crystallization in the shear flow.[50] Crystallization kinetics has been reviewed by Palberg for the hard-sphere systems.[51]

PHYSICO-CHEMICAL PROPERTIES

Static and Dynamic Light-Scattering Measurements

Figure 4 shows the static light-scattering intensity, $I(q)$ and the effective diffusion coefficients, estimated from the dynamic light-scattering, D_{eff}, as a function of scattering vector, q, for the colloidal silica spheres (diameter: 103 nm) at $\phi = 0.0049$.[52] Circles and crosses indicate the data for the suspensions with and without coexisted resins. The suspensions are "crystal" and "liquid," respectively. Surprisingly, very sharp peaks appeared for the crystals. The measurements have been made at intervals of half a degree. However, this interval was not always narrow enough for the determination of the reliable values of peak scattering vector, q_m. Static and dynamic light-scattering measurements have been made for various size of colloidal silica spheres[53,54] and polystyrene spheres.[55,56] It is interesting to note that the colloidal crystallization occurs for the monodispersed spheres larger than *ca.* 50 nm in diameter. For the smaller spheres structures were always "liquid."

The diffusion coefficients evaluated from the cumulative analysis are also shown in Figure 4. The D-values decreased as the scattering vector increased, whereas the background intensity of scattered light for the crystals increased as q increased. Furthermore, the diffusion coefficients from the suspensions showing peaks in the light-scattering curve were substantially low. According to Pusey and Tough,[57] the "effective diffusion coefficient," D_{eff} is given by

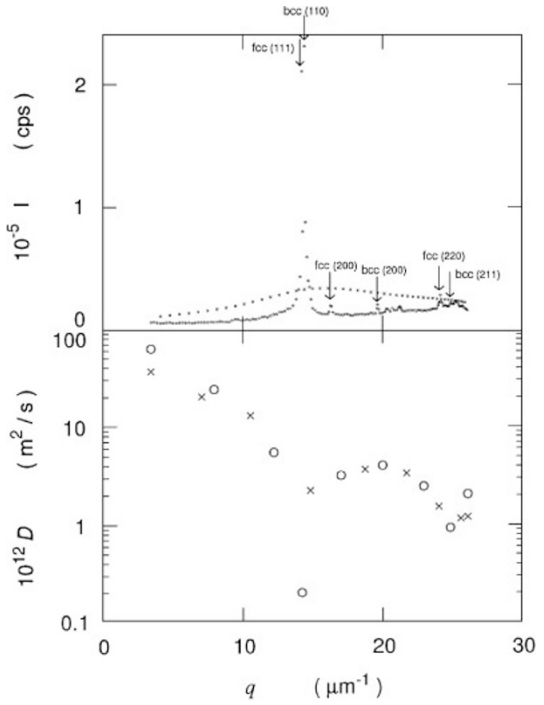

Figure 4. Light-scattering intensity and diffusion coefficient of colloidal crystals as a function of scattering vector at 24 °C.[52] $\phi = 0.0049$, ○: with resins, ×: without resins.

$$D_{eff} = D_o/S(q) \tag{10}$$

Where D_o is the diffusion coefficient of spheres in "gas" suspension and $S(q)$ is the structure factor. The constancy of $D_{eff} \times S(q)$ has been satisfactory for colloidal liquids, within experimental error. Figure 4 supports eq 10 as valid for colloidal systems.

Rigidity

The experimental results on the rigidity of colloidal crystals are summarized as follows.[11] First, the dynamic elastic modulus is always smaller than the static one. The meta-stable colloidal crystals are formed fast, *i.e.*, their structural relaxation times range from 10 ms to 1 s. However, the formation of the stable crystals in an equilibrium state requires a long time. The elasticity of the metastable crystals is low. Thus the dynamic moduli are smaller than the static rigidity in most cases. Figure 5 shows the plots of $\log G$ (rigidity) against $\log N$ (sphere number per unit volume) reported so far for some colloidal crystals of monodispersed polystyrene spheres with diameter ranging from 91 to 109 nm. G-values are denoted by open circles; crosses and open triangles are the static ones, which were evaluated by us at sedimentation equilibrium. The filled circles, filled squares and filled triangles denote dynamic rigidity.

Second, $\log G$ of colloidal crystals, including amorphous-solid, increases linearly with a slope of unity as $\log N$ increases. The order of magnitude of the modulus may be written in terms of the magnitude of the thermal fluctuation δ of a sphere as,

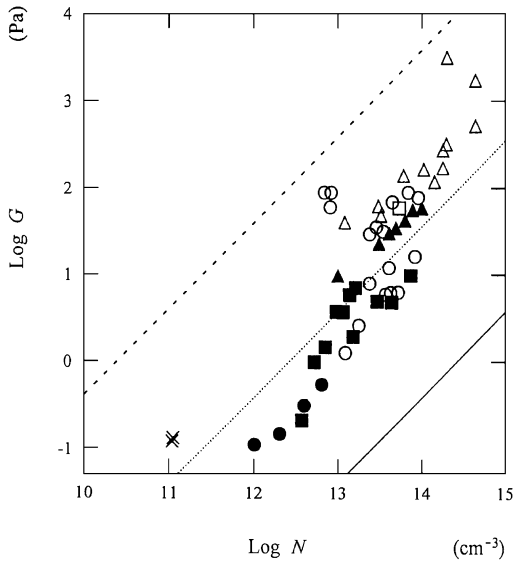

Figure 5. Plots of log G against log N for deionized polystyrene spheres. ○: reflection spectrum method in sedimentation equilibrium, △: rotatory viscometry, ×: microscopic method in sedimentation equilibtium, △: rotatory viscometry, □: reflection spectroscopy in an electric field, ●: Crandall and Williams, ▲: Mitaku *et al.*,[5] ■: Lindsay and Chaikin.[6]

$$G \sim f/l \sim (k_B T/\langle \delta^2 \rangle)/l \tag{11}$$

Where f is the force constant, l is the intersphere distance, and δ is the thermal fluctuation of a sphere in the effective potential valley. k_B and T are the Boltzmann constant and the temperature. Introducing a non-dimensional parameter g for $\langle \delta^2 \rangle^{1/2}/l$, the modulus is obtained as a linear function of N,

$$G \sim N k_B T/g^2 \tag{12}$$

When $g = 1$, eq 12 gives the rigidity of an ideal gas having the same sphere concentration. Lindemann's law of crystal melting tells us that $g < 0.1$ holds for a stable crystal.

Third, rigidity of the colloidal crystals, including amorphous-solid, is larger than that of colloidal liquid when comparisons are made at the same sphere concentration. Fourth, the rigidity of colloidal crystals increases substantially as the deionization of the suspension proceeds. Fifth, the rigidity of amorphous-solid increases as the polydispersity of spheres increases, and the G-value of the crystal is smaller than that of amorphous-solids at the same particle concentration. Sixth, rigidity of the structured suspensions increases as the charge density of the particles decreases, which is due to the extended electric double layers formed with the counter-ions of the particles. Seventh, rigidity at a certain concentration of particles first increases further. A maximum value of G was observed around 85 nm in diameter.

Recently, rigidity of colloidal alloys[58] and the colloidal crystals in alcoholic organic solvents[59] has been studied.

Viscosity and Viscoelasticity

This author has measured viscosities of colloidal liquids and crystals in exhaustively deionized aqueous suspensions, for the first time, with the use of an Ostwald-type viscometer and a rotational viscometer.[60–63] The viscosity of the deionized suspension was very sensitive to the degree of deionization of the suspension and decreased substantially when the suspension was contaminated with ionic species. The reduced viscosity, η_{sp}/c (specific viscosity, η_{sp}, divided by particle concentration, c) of colloidal liquids was much higher than that predicted by Einstein's equation and decreased sharply with increasing ion concentration. The specific viscosity of colloidal spheres can be given by eq 13.

$$\eta_{sp} = \eta/\eta_o - 1 = k_1\phi + k_2\phi_2 + \cdots. \tag{13}$$

Here η and η_o are the viscosities of the colloidal suspension and the solvent. ϕ is the concentration of the colloids (volume fraction). k_1 is the Einstein coefficient, 2.5; and k_2 denotes the electrostatic interaction parameter, which is very large for the deionized suspensions. The deviation of the observed η_{sp} values from Einstein's equation was very significant in the deionized liquids. However, the η_{sp} *vs.* ϕ relationship agreed very well with the Einstein equation in the presence of an excess amount of sodium chloride. Qualitatively speaking, the large k_2 observed implies that the electrostatic repulsion interaction is significant and the shells of the electrical double layers around the spheres are very thick. Furthermore, η_{sp}/c increased as the charge density decreased and/or the polydispersity index increased.

Viscometric properties of colloidal crystals are very peculiar. A sharp peak in the relative viscosity against concentration curves showing the phase transition between colloidal crystals and liquids was observed for the deionized spheres. A sharp increase in shear stress with increasing shear rate was observed for the colloidal crystals, from which the rigidity was evaluated as described in the preceding section. Furthermore, $\log \eta$ of colloidal crystals decreased linearly with a slope close to -1 as log [*shear rate*] increased. This supports strongly the solid-like nature of the suspensions. The $\log \eta$ *vs.* log [*shear rate*] plots for the colloidal liquids showed non-Newtonian flow with constant viscosity irrespective of shear rate.

Viscoelastic properties of colloidal liquids and crystals have been studied in detail.[64,65] The slopes of the log [*shear stress*] *vs.* log [*shear rate*] and/or log [*storage modulus*] *vs.* log [*angular frequency*] plots for the colloidal crystals were zero, and increased to unity as the structure transformed to liquids.

External Field Effects

The rigidity of colloidal crystals is very small, on the order of 10^{-2} to 10^3 Pa. On the other hand, those of metals are from 10^{10} to 10^{12} Pa. Thus, colloidal crystal is distorted very easily by the weak external fields, such as the gravitational field, shearing forces, an elevated pressure, an electric field, or centrifugal compression. The gravitational compression of colloidal crystals occurs easily. From the concentration dependence of the inter-sphere distance, at the bottom layer in the observation cell, the static elastic modulus can be determined in the sedimentation equilibrium.

Colloidal crystals in a rotating disk are also compressed in the centrifugal field.[66] Beautiful color bands appeared under the centrifugal field. The elastic moduli at various sphere concentrations can be obtained from the change in the reflection peak wavelengths as a function of the distance from the center in the centrifugal equilibrium. These color bands clearly show that the intersphere interactions are repulsive, and the repulsive forces are counter-balanced with the centrifugal fields.

Electric-force induced change in the lattice structure of colloidal crystals has been studied by several researchers.[11,20] The beautiful transformation effect of wave form from square to triangle has been observed.[67–75] This effect is explained by the fact that the translational motion of the charged spheres is too slow to follow up changes of the electric field.

Our research group observed second-order harmonics in the electro-optic effects of colloidal crystals. The frequency of the output was just twice that of the input field. In order to study the causes of the generation of the second-order harmonics, time-resolved reflection spectra were measured in a sine wave electric field. The peaks shifted shorter and then longer wavelengths periodically. Changes in the peak profiles, including the peak intensities and half-widths, were also observed clearly under a sine wave electric field. Plots of the peak wavelengths were plotted against time. The frequency observed was the same as that applied. However, the integrated intensities of the reflection peak profile for the whole change of wavelengths were modulated drastically, and the frequency was just twice the one applied. In other words, second-order harmonics were obtained for the integrated intensity. The calculation of the integrated intensities is quite consistent with observation using the photomultiplier. The observed harmonics were caused by the nature of colloidal crystals themselves.

The amplitudes, *a.c.* components of the electrically induced shear waves as a function of the frequency applied, showed several peaks in the curves. The peak shifted to the higher frequencies as sphere concentration increased. The appearance of the peaks demonstrates the existence of some characteristic frequencies for the viscoelastic colloidal crystals. We observed the harmonic oscillation on the shear waves of colloidal crystals from electro-optical effects using electric light scattering measurements. At 90 degrees scattered light is detected from incident white light. The *synchronous oscillation* remains even after the sine wave electric current was turned off. This is due to the sheared waves of the crystals. Photonic-trapping effect of colloidal crystals has been studied.[75]

Recently, photonic band gap (PBG) or photonic crystal has been developed. Structure exhibiting full photonic band gap in the microwave, millimeter and sub-millimeter regimes have been fabricated more than ten years ago. Now, submicron length-scale photonic crystal has been developed rapidly using colloidal crystals as the starting material.[76–84] Two-dimensional ordering induced by the electric field has been reported by several research groups.[85–87] Crystal-liquid phase transition induced by ultraviolet light irradiation was reported for colloidal suspension containing malachite green.[88]

The deformation of colloidal crystals by the shearing forces, high pressure, foreign salt, and/or other additives such as water-soluble polymers, has been studied by several researchers.[20] Thermo-sensitive colloidal crystals have been made using hydrogel of *N*-isopropylacrylamide.[89–92]

CONCLUSIONS

Colloidal crystals are the suspensions in which colloidal particles distribute regularly as atoms and molecules do in metals and protein crystals. Giant colloidal crystals were found by the authors emit brilliant iridescent colors by the Bragg diffraction and are quite beautiful. In this article, recent works in our laboratory on the structural colors, morphology, crystallization kinetics, structural and dynamic properties and the electro-optic effects of colloidal crystals have been discussed. Formation of giant colloidal crystals is due to the electrostatic intersphere repulsion and to the highly expanded electrical double layers surrounding colloidal spheres.

Received: October 20, 2007
Accepted: April 24, 2008
Published: June 18, 2008

REFERENCES

1. W. Vanderhoff, H. J. van de Hul, R. J. M. Tausk, and J. Th. G. Overbeek, in "Clean Surfaces: Their Preparation and Characterization for Interfacial Studies," G. Goldfinger, Ed., Marcel Dekker, New York, 1970, p 15.
2. P. A. Hiltner, Y. S. Papir, and I. M. Krieger, *J. Phys. Chem.*, **75**, 1881 (1971).
3. A. Kose, M. Ozaki, K. Takano, Y. Kobayashi, and S. Hachisu, *J. Colloid Interface Sci.*, **44**, 330 (1973).
4. R. Williams, R. S. Crandall, and P. J. Wojtowicz, *Phys. Rev. Lett.*, **37**, 348 (1976).
5. S. Mitaku, T. Ohtsuki, A. Kishimoto, and K. Okano, *Biophys. Chem.*, **11**, 411 (1980).
6. H. M. Lindsay and P. M. Chaikin, *J. Chem. Phys.*, **76**, 3774 (1982).
7. P. Pieranski, *Contempt. Phys.*, **24**, 25 (1983).
8. R. H. Ottewill, *Phys. Chem.*, **89**, 517 (1985).
9. D. J. W. Aastuen, N. A. Clark, L. K. Cotter, and B. J. Ackerson, *Phys. Rev. Lett.*, **57**, 1733 (1986).
10. P. N. Pusey and W. van Megen, *Nature (London)*, **320**, 340 (1986).
11. T. Okubo, *Acc. Chem. Res.*, **21**, 281 (1988).
12. W. B. Russel, D. A. Saville, and W. R. Schowalter, "*Colloidal Dispersions*," Cambridge University Press, Cambridge, 1989, p 329.
13. A. K. Sood, *Solid State Phys.*, **45**, 2 (1991).
14. B. J. Ackerson and N. A. Clark, *Phys. Rev. Lett.*, **46**, 123 (1981).
15. T. Okubo, *J. Chem. Soc. Faraday Trans.*, **1**, 84, 1163 (1988).
16. Y. Monovoukas and A. P. Gast, *J. Colloid Interface Sci.*, **128**, 533 (1989).
17. D. J. W. Aastuen, N. A. Clark, J. C. Swindall, and C. D. Muzny, *Phase Transitions*, **21**, 139 (1990).
18. T. Okubo, *J. Chem. Phys.*, **95**, 3690 (1991).
19. T. Okubo, *Naturwissenschaften*, **79**, 317 (1992).
20. T. Okubo, *Prog. Polym. Sci.*, **18**, 481 (1993).
21. R. Simon, T. Palberg, and P. Leiderer, *J. Chem. Phys.*, **99**, 3030 (1993).
22. T. Okubo, *Colloid Polym. Sci.*, **271**, 190 (1993).
23. T. Okubo, *Langmuir*, **10**, 1695 (1994).
24. T. Okubo, *Langmuir*, **10**, 3529 (1994).
25. (a) T. Okubo, in "Macro-ion Characterization. From Dilute Solutions

to Complex Fluids," K. S. Schmitz, Ed., Am. Chem. Soc., Washington, D. C., 1994, p 364.
(b) T. Okubo and A. Tsuchida, *Forma*, **17**, 141 (2002).
(c) T. Okubo, in "Structural Colors in Biological Systems," S. Kinoshita and S. Yoshioka, Ed., Osaka University Press, 2005, p 267.
26. T. Okubo, H. Yoshimi, T. Shimizu, and R. H. Ottewill, *Colloid Polym. Sci.*, **278**, 469 (2000).
27. W. B. Russel, *Phase Transition*, **21**, 127 (1990).
28. C. R. Harkless, M. A. Singh, S. E. Nagler, G. B. Stephenson, and J. L. Jordan-Sweet, *Phys. Rev. Lett.*, **64**, 2285 (1990).
29. J. K. G. Dhont, C. Smits, and H. N. W. Lekkerkerker, *J. Colloid Interface Sci.*, **152**, 386 (1992).
30. K. Schätzel and B. J. Ackerson, *Phys. Rev. E*, **48**, 3766 (1993).
31. N. Würth, J. Schwarz, F. Culis, P. Leidener, and T. Palberg, *Phys. Rev. E*, **52**, 6415 (1995).
32. W. van Megen, *Transport Theor. Stat. Phys.*, **24**, 1017 (1995).
33. W. M. Itano, J. J. Bolinger, J. N. Tan, B. Jelenkovic, X. P. Huang, and D. J. Wineland, *Science*, **279**, 686 (1998).
34. (a) T. Okubo, *Ber. Bunsen-Ges. Phys. Chem.*, **91**, 516 (1987).
(b) T. Okubo, *Colloid Polym. Sci.*, **285**, 245 (2006).
35. T. Okubo, *Angew. Chem., Int. Ed. Engl.*, **26**, 765 (1987).
36. T. Okubo and S. Aotani, *Naturwissenschaften*, **75**, 145 (1988).
37. (a) T. Okubo and S. Aotani, *Colloid Polym. Sci.*, **266**, 1049 (1988).
(b) A. B. D. Brown, S. M. Clarke, and A. R. Rennie, *Langmuir* **14**, 3129 (1998).
38. (a) T. Okubo, H. Kimura, H. Hase, K. Yamaguchi, and K. Nagai, *Colloid Polym. Sci.*, **282**, 250 (2004).
(b) T. Okubo, H. Kimura, H. Hase, P. A. Lovell, N. Erington, and P. Thongnoi, *Colloid Polym. Sci.*, **283**, 393 (2005).
(c) J. Okamoto, H. Kimura, A. Tsuchida, T. Okubo, and K. Ito, *Colloids Surf., B. Biointerface*, **56**, 231 (2007).
39. J. Zhu, M. Li, R. Reger, W. Meyer, R. H. Ottewill, STS-73 Space Shuttle Crew, W. B. Russel, and P. M. Chaikin, *Nature (London)*, **387**, 883 (1997).
40. T. Okubo, S. Okada, and A. Tsuchida, *J. Colloid Interface Sci.*, **189**, 337 (1997).
41. T. Okubo and S. Okada, *J. Colloid Interface Sci.*, **192**, 490 (1997).
42. T. Okubo, A. Tsuchida, and T. Kato, *Colloid Polym. Sci.*, **277**, 191 (1999).
43. T. Okubo and H. Ishiki, *J. Colloid Interface Sci.*, **228**, 151 (2000).
44. T. Okubo, *J. Chem. Soc., Faraday Trans. 1*, **82**, 3163 (1986).
45. E. M. Wong, J. E. Bonevich, and P. C. Pearson, *J. Phys. Chem. B*, **102**, 7770 (1998).
46. T. Okubo and S. Okada, *J. Colloid Interface Sci.*, **204**, 198 (1998).
47. (a) T. Okubo, H. Ishiki, H. Kimura, M. Chiyoda, and K. Yoshinaga, *Colloid Polym. Sci.*, **280**, 290 (2002).
(b) K. Yoshinaga, M. Chiyoda, H. Ishiki, and T. Okubo, *Colloids Surf., A*, **204**, 285 (2002).
48. (a) T. Okubo, A. Tsuchida, T. Okuda, K. Fujitsuna, M. Ishikawa, T. Morita, and T. Tada, *Colloids Surf. A*, **160**, 311 (1999).
(b) T. Okubo, A. Tsuchida, K. Kobayashi, A. Kuno, T. Morita, M. Fujitsuna, and Y. Kohno, *Colloid Polym. Sci.*, **277**, 474 (1999).
(c) A. Tsuchida, K. Taguchi, E. Takyo, H. Yoshimi, S. Kiriyama, T. Okubo, and M. Ishikawa, *Colloid Polym. Sci.*, **278**, 872 (2000).
(d) T. Okubo and A. Tsuchida, *Ann. N. Y. Acad. Sci.*, **974**, 164 (2002).
49. T. Okubo, A. Tsuchida, S. Takahashi, K. Taguchi, and M. Ishikawa, *Colloid Polym. Sci.*, **278**, 202 (2000).
50. A. Tsuchida, E. Takyo, K. Taguchi, and T. Okubo, *Colloid Polym. Sci.*, **282**, 1105 (2004).
51. T. Palberg, *J. Phys. Condens. Matter*, **11**, 323 (1999).
52. T. Okubo, K. Kiriyama, N. Nemoto, and H. Hashimoto, *Colloid Polym. Sci.*, **272**, 93 (1996).
53. T. Okubo and K. Kiriyama, *J. Mol. Liq.*, **72**, 347 (1997).
54. T. Okubo and A. Tsuchida, *Colloid Polym. Sci.*, **280**, 438 (2002).
55. T. Okubo and K. Kiriyama, *Ber. Bunsen-Ges. Phys. Chem.*, **100**, 849 (1996).
56. T. Okubo, K. Kiriyama, H. Yamaoka, and N. Nemoto, *Colloids Surf. A*, **103**, 47 (1995).
57. P. N. Pusey and R. J. A. Tough, in "Particle Interactions. Dynamic Light Scattering," R. Pecora, Ed., Plenum, London, 1985, p 85.
58. T. Okubo and H. Ishiki, *Colloid Polym. Sci.*, **279**, 571 (2001).
59. T. Okubo, H. Ishiki, H. Kimura, M. Chiyoda, and K. Yoshinaga, *Colloid Polym. Sci.*, **280**, 290 (2002).
60. T. Okubo, *J. Chem. Phys.*, **87**, 6733 (1987).
61. T. Okubo, *Ber. Bunsen-Ges. Phys. Chem.*, **92**, 504 (1988).
62. T. Okubo, *J. Phys. Chem.*, **94**, 1962 (1990).
63. T. Okubo, *Colloid Polym. Sci.*, **271**, 873 (1993).
64. T. Matsumoto and T. Okubo, *J. Rheol.*, **35**, 135 (1991).
65. (a) T. Okubo, H. Kimura, T. Hatta, and T. Kawai, *Phys. Chem. Chem. Phys.*, **4**, 2260 (2002).
(b) H. Kimura and T. Okubo, *Colloid Polym. Sci.*, **280**, 579 (2002).
(c) T. Okubo, H. Kimura, T. Kawai, and H. Niimi, *Langmuir*, **19**, 6014 (2003).
(d) H. Kimura, H. Niimi, A. Tsuchida, and T. Okubo, *Colloid Polym. Sci.*, **283**, 1079 (2005).
(e) H. Kimura, Y. Nakayama, A. Tsuchida, and T. Okubo, *Colloids Surf., B: Biointerface*, **56**, 236 (2007).
66. T. Okubo, *J. Am. Chem. Soc.*, **112**, 5420 (1990).
67. (a) M. Stoimenova and T. Okubo, *J. Colloid Interface Sci.*, **176**, 267 (1995).
(b) M. Stoimenova, V. Dimitrov, and T. Okubo, *J. Colloid Interface Sci.*, **184**, 106 (1996).
68. T. Okubo, A. Tsuchida, S. Okada, and S. Kobata, *J. Colloid Interafce Sci.*, **199**, 83 (1998).
69. T. Okubo, A. Tsuchida, T. Takahashi, and A. Iwata, *J. Colloid Interafce Sci.*, **207**, 130 (1998).
70. T. Okubo, A. Tsuchida, A. Iwata, and T. Takahashi, *Colloids Surf., A*, **148**, 87 (1999).
71. M. Stoimenova, A. Alekov, and T. Okubo, *Colloids Surf., A*, **148**, 83 (1999).
72. M. Stoimenova and T. Okubo, in "Surfaces of Nanoparticles and Porous Materials," J. A. Schwarz and C. I. Contescu, Ed., Marcel Dekker, New York, 1999, p 103.
73. A. Tsuchida, T. Taniguchi, T. Tanahashi, and T. Okubo, *Langmuir*, **15**, 4203 (1999).
74. (a) T. Okubo, *Prog. Colloid Polym. Sci.*, **124**, 112 (2003).
(b) A. Tsuchida, K. Shibata, and T. Okubo, *Colloid Polym. Sci.*, **281**, 1104 (2003).
(c) K. Shibata, H. Kimura, A. Tsuchida, T. Okubo, S. Sato, and K. Yoshinaga, *Colloid Polym. Sci.*, **284**, 372 (2006).
(d) A. Tsuchida and T. Okubo, in "Molecular and Colloidal Electro-optics," S. Stoylov and M. Stoimenova, Ed., CRC Press, 2006, p 447.
75. (a) K. Shibata, T. Yamamoto, M. Kurita, H. Kimura, A. Tsuchida, and T. Okubo, *Colloid Polym. Sci.*, **284**, 688 (2006).
(b) K. Shibata, H. Kimura, A. Tsuchida, and T. Okubo, *Colloid Polym. Sci.*, **285**, 127 (2006).
76. R. D. Pradhan, J. A. Bloodgood, and G. H. Watson, *Phys. Rev. B*, **55**, 9503 (1997).
77. J. E. G. Wijnhoven and W. L. Vos, *Science*, **281**, 802 (1998).
78. A. A. Zakhidov, R. H. Baughman, Z. Igbal, C. Culi, I. Khayrullin, S. O. Dantas, J. Marti, and V. G. Ralchenko, *Science*, **282**, 897 (1998).
79. B. G. Levi, *Phys. Today*, **12**, 21 (1999).
80. M. Megen, J. E. G. Wijnhoven, A. Lagendijk, and W. L. Vos, *J. Opt. Soc. Am. B*, **16**, 1403 (1999).
81. S. H. Park and Y. Xia, *Langmuir*, **15**, 266 (1999).
82. J. D. Debord and L. A. Lyon, *J. Phys. Chem. B*, **104**, 6327 (2000).
83. M. Freemantle, *Chem. Eng. News*, **55** (2001).
84. M. Shim, C. Wang, and P. Guyot-Sionnest, *J. Phys. Chem. B*, **105**, 2369 (2001).
85. M. Trau, D. A. Saville, and I. A. Aksay, *Science*, **272**, 706 (1996).
86. B. M. I. van der Zande, G. J. M. Koper, and H. N. W. Lekkerkerker, *J. Phys. Chem.*, **103**, 5754 (1999).
87. T. Gong and D. W. M. Marr, *Langmuir*, **17**, 2301 (2001).

88. Z. Z. Gu, A. Fujishima, and O. Sato, *J. Am. Chem. Soc.*, **122**, 12387 (2000).
89. H. Senff and W. Richtering, *J. Chem. Phys.*, **111**, 1705 (1999).
90. R. Pelton, *Adv. Colloid Interface Sci.*, **85**, 1 (2000).
91. Z. Hu, X. Lu, and J. Gao, *Adv. Mater.*, **13**, 1708 (2001).
92. (a) T. Okubo, H. Hase, H. Kimura, and E. Kokufuta, *Langmuir*, **18**, 6783 (2002).
(b) T. Okubo, T. Mizutani, J. Okamoto, K. Kimura, A. Tsuchida, K. Tauer, V. Khrenov, H. Kawaguchi, and S. Tsuji, *Colloid Polym. Sci.*, **285**, 351 (2006).

Tsuneo OKUBO was born in Tsubame, Niigata, Japan, in 1941, and graduated from the Department of Fiber Chemistry of Kyoto University, Japan in 1964. He studied polymer physics and awarded Master of Engineering in 1966 and Doctor of Engineering in 1971 at the same university. He joined the Department of Polymer Chemistry as a Research Assistant in 1969 and was appointed Associate Professor in 1978 at the same Department. He was a research associate with Professor N. J. Turro at Columbia University, USA in 1978 and 1979. He was promoted to full Professor at the Department of Applied Chemistry of Gifu University in 1996. He retired from the Gifu University and was appointed Professor Emeritus from the same university in 2004. He founded the Institute of Colloidal Organization at Kyoto in 2004 and the Head Professor of the Institute. He was also appointed Guest Professor at the Graduate School of Engineering of Yamagata University in 2004. He was awarded the Polymer Science Award in 1978. He is the Chair of International Advisory Board of ELOPTO (Electro-optics) Series since 2006. He is appointed an Editorial Board of the international journal, Colloid Polymer Science in 2008. His research interests include the physical chemistry of polyelectrolyte solutions & colloidal suspensions, colloidal crystals, and dissipative structural patterns of solutions & suspensions.

